

DAUBECHIES COMPLEX WAVELET TRANSFORM BASED MULTILEVEL SHRINKAGE FOR DEBLURRING OF MEDICAL IMAGES IN PRESENCE OF NOISE

ASHISH KHARE

*Department of Electronics and Communication
University of Allahabad, Allahabad, 211002, India
khare@allduniv.ac.in
ashishkhare@hotmail.com*

UMA SHANKER TIWARY

*Indian Institute of Information Technology
Allahabad, 211011, India
ust@iita.ac.in*

MOONGU JEON*

*Department of Information and Communication
Gwangju Institute of Science and Technology
Gwangju, 500712, Republic of Korea
mjjeon@gist.ac.kr*

Received 22 May 2008
Revised 27 October 2008

Deblurring in the presence of noise is a hard problem, especially in ultrasonic and CT images. In this paper, we propose a new method of image deblurring in presence of noise, using symmetric Daubechies complex wavelet transform. The proposed method is based on shrinkage of multilevel Daubechies complex wavelet coefficients, and is adaptive as it uses shrinkage function based on the variance of wavelet coefficients as well as the mean and the median of absolute wavelet coefficients at a particular level. The results obtained after the application of the proposed method demonstrate an improved performance over other related methods available in literature.

Keywords: Daubechies complex wavelet transform; deconvolution; colored noise removal; multilevel thresholding; medical image deblurring.

AMS Subject Classification: 22E46, 53C35, 57S20

*Corresponding author.

1. Introduction

The major challenge of medical imaging science is to provide a way to enable faithful extraction of scientific and clinical information. The images obtained from medical instruments are generally of poor contrast and corrupted by blur and noise due to applications of various quantization, reconstruction and enhancement algorithms. For example, an ultrasound image can be viewed as a distorted version of original image, where the distortion operator is a convolution with a point spread function (PSF) of the imaging system.¹ Wagner *et al.*² suggested a special PSF, called scatter PSF for modeling blur in X-ray image. Images like PET and SPECT are also reported to be blurred.^{3,4} Recently it has been shown that CT scanners cannot resolve many important bone details, especially those of millimeter or sub-millimeter sized features due to presence of blur.⁵ In this context, deblurring is an effective strategy⁵ to resolve these minute details. These blurred images are often corrupted with various types of noise, for example, ultrasonic images are assumed to contain speckle noise and CT images are supposed to be corrupted by Poisson distributed random noise.⁶ Corruption of blurred images with noise makes them poor for visual analysis.

Sparseness, decorrelation and locality properties of wavelets make them very useful for blur as well as noise removal⁷ from images. Although real-valued wavelet transform based techniques have given good results, but real-valued wavelet transform suffers from two serious disadvantages.⁷⁻¹¹ (i) its shift-sensitive nature and (ii) no phase information. Recently a few attempts¹² have been made for shift-invariant deblurring but the use of cycle-spinning make them computationally costly. To achieve shift-invariance, stationary wavelet transform¹³ can also be used, but again this transform is computationally costly and it does not provide phase information as well. The use of complex-valued wavelet transform (CxWT) can minimize both the shortcomings of real-valued discrete wavelet transform (DWT).⁷⁻¹¹ The complex wavelet transform has not been explored much when compared to the DWT. From the implementation point of view, complex wavelet transform can be implemented in different ways. For constructing an approximately shift-invariant redundant wavelet transform, Gopinath¹⁴ has given the concept of phaselet transform that includes the Kingsbury's Dual Tree Complex Wavelet Transform^{8,15,16} as a special case. Fernandes⁹ has developed a framework of one dimensional mapping based CxWT on controllable redundancy while Bharath¹⁷ constructed steerable pyramid complex wavelet transform. These complex wavelet transform uses real filters instead of complex filters. Lawton¹⁸ and Lina-Mayrand¹⁹ have proposed complex Daubechies wavelets, which is a natural extension of the real Daubechies wavelets.

During the deblurring of an image in presence of noise, the application of pseudo-inverse filter or its variants introduce colored noise in the image. A few authors dealt with this problem in real wavelet domain. Donoho²⁰ suggested wavelet-vagulette deconvolution (WVD) algorithm, which uses vagulette that can simultaneously

invert the data and perform wavelet transform. After computing wavelet coefficients, the coefficients were shrunk by a certain parameter and inverse wavelet transform of shrunk coefficients give the estimate of deblurred image. A mirror wavelet based deconvolution for solving inverse problems was given by Kalifa *et al.*²¹ Kalifa–Mallat²² have done a study on various wavelet thresholding estimators for the linear inverse problem and deconvolution. A theoretical analysis for solving deconvolution problem in wavelet domain is given by Fan and Koo.²³ Guo *et al.*²⁴ proposed a method for restoration of blurred noisy images without any prior knowledge of the blurring function and the statistics of noise. Their proposed method²⁴ combine wavelet transform with radial basis function (RBF) neural network to restore the given image. Recently Neelamani *et al.*²⁵ had developed a method which applies regularized inverse filter followed by shrinkage in Fourier as well as wavelet domain, as Fourier domain represent information of colored noise economically. An iterative regularization method in translation invariant wavelet transform based denoising has been proposed by Li *et al.*²⁶ for better denoising effect. Jhonstone *et al.*²⁷ developed a simple method in which colored noise is removed by applying multilevel hard thresholding in wavelet domain using Meyer wavelet. Much improved version of Johnstone’s method²⁷ is given by Donoho–Raimondo,¹² for achieving translation invariant deblurring.

A novel method for blur removal from blurred and noisy images, where unknown type of noise is present, is proposed in the present paper, which is based on shrinkage of wavelet coefficients in multilevel^{6,7,34,35} Daubechies complex wavelet domain. The proposed method has been compared with earlier state-of-art deconvolution methods: Fourier-Wavelet Regularized Deconvolution (ForWaRD)²⁵ and Translation-Invariant Wavelet Deconvolution (TI-WaveD),¹² based on real wavelet transform. The results have also been compared with the traditional Wiener filter.

The rest of the paper is organized as follows: we briefly described the basic concepts of Daubechies complex wavelet transform and its properties in Sec. 2. Details of the proposed method are given in Sec. 3. In Sec. 4, the results after the application of the proposed method for deblurring in presence of noise are shown and they are compared with other methods with respect to mean square error (MSE), signal-to-noise ratio (SNR) and wavelet based blur measure (W). Finally in Sec. 5 conclusions are given.

2. Daubechies Complex Wavelet Transform

The basic equation of multiresolution theory is the scaling equation

$$\phi(t) = 2 \sum_n a_n \phi(2t - n). \quad (2.1)$$

where a_n ’s are coefficients. The a_n ’s can be real as well as complex valued and $\sum a_n = 1$. Daubechies’s wavelet bases $\{\psi_{j,k}(t)\}$ in one dimension are defined through the above scaling function and multiresolution analysis of $L_2(\mathfrak{R})$.²⁸ During

the formation of general solution, Daubechies considered a_n to be real-valued only. Relaxing the condition for a_n to be only real-valued will lead to Daubechies complex scaling function and this leads to complex Daubechies wavelet transform. The construction of complex Daubechies wavelet has been done as in Lina and Mayrand.¹⁹ The generating wavelet $\psi(t)$ is given by,

$$\psi(t) = 2 \sum_n (-1)^n \overline{a_{1-n}} \phi(2t - n). \tag{2.2}$$

Here $\psi(t)$ and $\phi(t)$ share the same compact support $[-N, N + 1]$.

Any function $f(t)$ can be decomposed into complex scaling function and mother wavelet as:

$$f(t) = \sum_k c_k^{j_0} \phi_{j_0,k}(t) + \sum_{j=j_0}^{j_{\max}-1} d_k^j \psi_{j,k}(t). \tag{2.3}$$

where, j_0 is a given resolution level, $\{c_k^{j_0}\}$ and $\{d_k^j\}$ are known as approximation and detail coefficients. The Daubechies complex wavelet function can be made symmetric.¹⁰ We have used Symmetric Daubechies complex Wavelet (SDW) transform.¹⁰ The Symmetric Daubechies complex Wavelet transform has the following advantages:

- (i) It has perfect reconstruction property.
- (ii) No redundancy: Other popular CxWT like DTCWT¹¹ has a redundancy of $2^m : 1$ for m -dimensional signal, while Daubechies CxWT has no such redundancy.
- (iii) Number of computations in Daubechies CxWT (although it involves computation on complex numbers) is same as that of DWT, while DTCWT have 2^m times computations as that of DWT for an m -dimensional signals.
- (iv) It is symmetric. This property makes it easy to handle edge points during the signal reconstruction.

All the usual properties of real Daubechies wavelet bases are derived from the amplitude.²⁸ Thus those properties are maintained in the complex solution. However, complex Daubechies wavelets exhibit two other important properties as follows.

2.1. Reduced shift sensitivity

Daubechies complex wavelet transform is approximately shift invariant. A transform is shift sensitive if an input signal shift causes an unpredictable change in transform coefficients. In DWT shift sensitivity arises from downsampling in the implementation. Figure 1 shows a circular edge structure reconstructed using real and complex Daubechies wavelets at single scale. From Fig. 1, it is clear that as the circular edge structure moves through space, the reconstruction using real valued DWT coefficients changes erratically, while complex wavelet transform reconstructs all local shifts and orientations in the same manner.²⁹ From Fig. 1, it is also clear that Daubechies complex wavelet transform is rotational invariant.

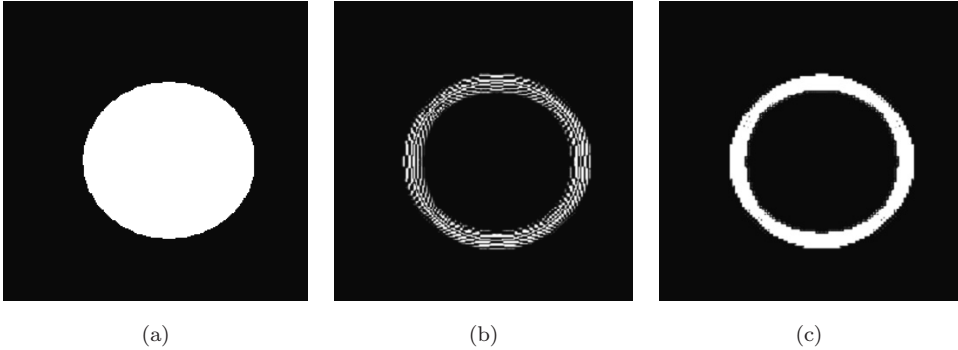


Fig. 1. (a) A circular edge structure, (b) reconstructed using real-valued DWT at single scale and (c) reconstructed using Daubechies complex wavelet transform at single scale.

2.2. Availability of phase information

The phase of an image plays an important role in many coherent image processing applications like ultrasonography. The phase of complex wavelet coefficients represents the skeleton of the signal. Two dimensional DWT does not provide phase information at all. The results presented in Clonda¹⁰ suggest that the magnitude and the phase of wavelet coefficients are collaborating in non-trivial way to describe the data. The phases encode most of the coherent (in space and scale) structure of the image while the modulus mostly encodes the strength of local information that could be corrupted with noise. The complete understanding of informational content of the phase of wavelet coefficients is still an open problem.

3. The Proposed Model

3.1. The problem and the related work

The image observation model is represented as

$$y = h * x + n \quad (3.1)$$

where y is an observed image consisting of degradation of unknown desired image x by circular convolution (denoted by $*$) with a point spread function of impulse response h and n is the amount of noise. The objective is to recover x from known y . Simple denoising followed by deblurring will distort the image and create blocking artifacts,³⁰ while simple deblurring creates a complicated noise structure.²⁵ If the noise is Gaussian additive then the problem is comparatively easier and some literatures are available for wavelet based deconvolution in the presence of Gaussian noise.^{12,20–23,25,27} However, if the noise is non-Gaussian then the problem becomes very difficult and a few literature deal with blur removal in presence of salt-and-pepper noise.³⁰ In Fourier domain, the observation model given by Eq. (3.1) is

$$Y = HX + N \quad (3.2)$$

where Y , H , X and N are discrete Fourier transforms of the observations y , impulse response h , desired signal x and noise n .

If the system frequency response H is invertible, an unbiased estimate of x can be obtained in Fourier domain,

$$\tilde{X} = H^{-1}Y = X + H^{-1}N. \quad (3.3)$$

However, if H is very small, the noise is enormously amplified, which yields an extremely noisy estimate. Here the term $H^{-1}N$ introduces colored noise in the image. Thus the problem is an ill-posed inverse problem, as the noise contaminates the data and the inversion process strongly amplifies the noise. Noise amplification can be alleviated by using an approximated, regularized inverse filter instead of a pure inverse filter. Regularization aims to provide a better solution by reducing noise in exchange for some bias in the estimate and becomes essential in situations involving ill-conditioned systems. Most of wavelet based deconvolution approaches attempt to use shrinkage function to remove colored noise.^{12,25,27}

The important contributions for wavelet based deconvolution problem are WVD,²⁰ ForWaRD²⁵ and WaveD.²⁷ All of these methods work in two stages — deblurring followed by removal of colored noise. WVD algorithm employs a scale dependent universal threshold to estimate the signal wavelet coefficients. Unfortunately, WVD was designed to deconvolve only a limited class of scale invariant systems. ForWaRD applies Fourier domain shrinkage after computing pseudo-inverse filter estimate followed by wavelet domain shrinkage. The performance of ForWaRD is good only for Boxcar blur with low noise levels. WaveD uses Meyer wavelet for computing wavelet transform. It applies hard thresholding on wavelet coefficients by computing threshold at multiple levels. One modification in WaveD has been done by Donoho and Raimondo.¹² They proposed translation-invariant wavelet deconvolution (TI-WaveD) for getting translation invariant deblurred estimate. The limitation of WaveD and TI-WaveD is dependence of their performance on tuning of some parameters. Also TI-WaveD is computationally costly due to use of cycle-spinning.

3.2. *The method*

The white noise is uniformly distributed across the subbands, while the image transform concentrates over a small number of coefficients. Figure 2 shows the fact that the wavelet transform corresponding to the actual image gives a small number of significant wavelet coefficients. If we consider deconvolution as a denoising problem, then we have to deal with colored noise. It has been shown in Fig. 3 that the high frequency subbands are contaminated by the deconvolved noise, so that the signal present in these subbands is not recoverable by any simple thresholding method.³¹

We have proposed a method, which applies pseudo inverse filter in Fourier domain. Colored noise due to application of pseudo inverse filter can be removed by

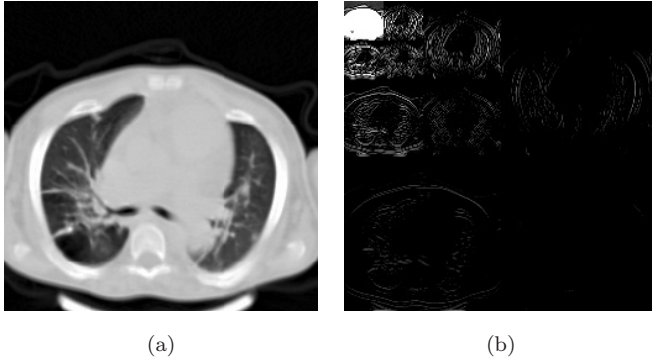


Fig. 2. (a) An image and (b) magnitude of complex wavelet transform of the image.

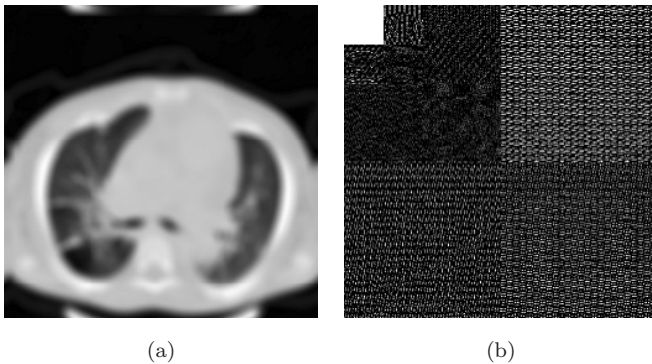


Fig. 3. (a) Blurred image and (b) magnitude of complex wavelet transform of the image deconvolved without regularization.

multilevel thresholding of the complex wavelet coefficients. The proposed method works in two stages — deblurring followed by the residual noise removal.

3.2.1. Deblurring

Apply the pseudo-inverse filter in Fourier domain, to get \tilde{X} , an estimate of X in Fourier domain, as in (3.3),

$$\tilde{X} = \begin{cases} X + \frac{N}{H}, & \text{if } |H| > 0 \\ 0, & \text{otherwise} \end{cases}. \tag{3.4}$$

Inverse Fourier transform of \tilde{X} gives deblurred estimate \tilde{x} . Here the term N/H causes colored noise in deblurred estimate which is removed in the next stage.

3.2.2. Noise removal

Recently we have proposed a multilevel adaptive threshold^{6,7} and a soft-shrinkage function, which depends on three statistical parameters of complex wavelet coefficients: the variance of wavelet coefficients, the mean and the median of absolute wavelet coefficients at a particular level. The theoretical derivation of soft-shrinkage function has been given in the Appendix. It has been shown^{6,7} that the proposed threshold is capable of removing the signal dependent as well as signal independent noise. We extended our proposed multilevel threshold based denoising framework to remove colored noise in complex wavelet domain. Our proposed method for colored noise removal is as follows:

- (i) Compute symmetric Daubechies complex wavelet transform of pseudo inverse filtered estimate \tilde{x} , called w .
- (ii) Set the level-dependent threshold

$$T_j = \frac{1}{2^{j-1}} \left(\frac{\sigma}{\mu} \right) M \quad (3.5)$$

where j is resolution level, σ is the standard deviation of wavelet coefficients, μ and M are the mean and the median of absolute wavelet coefficients at the j th level for a particular subband.

- (iii) Compute the soft-shrinkage function

$$f(\sigma) = \begin{cases} 0, & \text{if } |w| \leq T \\ \left(1 - \frac{T^2}{w^2}\right), & \text{if } |w| > T \end{cases} \quad (3.6)$$

Apply this soft-shrinkage function on magnitude of complex wavelet coefficients (w) to get $\tilde{w} = f(\sigma).w$, as discussed in the Appendix, using computed threshold of Eq. (3.5), at different resolution levels. Retain the phase component of complex wavelet coefficients.

- (iv) Apply inverse wavelet transform on shrunk wavelet coefficients to obtain the denoised image.

Our proposed multilevel algorithm is fully adaptive and the parameters depend on the blurred and noisy image. This algorithm also enjoys the translation-invariance due to the use of complex wavelet transform. The algorithm can deblur the blurred images corrupted by signal dependent non-Gaussian as well as signal independent Gaussian noise.

4. Experiments and Results

Here we present the results of the proposed method and compared our results with other popular methods. We have performed our experiments on simulated 256×256 medical images. As a quantitative performance measure the mean square

error (MSE),³³ the signal to noise ratio (SNR)³³ and the wavelet based blur measure (W)³² has been used. The wavelet based blur measure (W) is defined as,

$$W = \sqrt{\frac{\|h_w(x)\|^2}{\|x\|^2 - \|h_w(x)\|^2}}$$

where $h_w(x)$ are the high pass wavelet coefficients of signal x . Because of norm preservation in the wavelet based blur measure (W), blurring of image decreases the energy in the high pass bands and simultaneously increases the energy in the low pass bands, so the measure, W, decreases by increasing the blur amount.

For one representative case, the findings of our proposed method is shown in Fig. 4 which shows the visual superiority of the proposed method over the Weiner filter,³³ ForWaRD²⁵ and TI-WaveD¹² on one representative reference image. For this we have added a small amount of noise and blur in the reference image and then restored image is estimated by the Weiner filter, the ForWaRD, the TI-WaveD and the proposed method. By means of experiments, we found that the proposed new multilevel algorithm gives good results at 7–10 resolution levels. In all the results

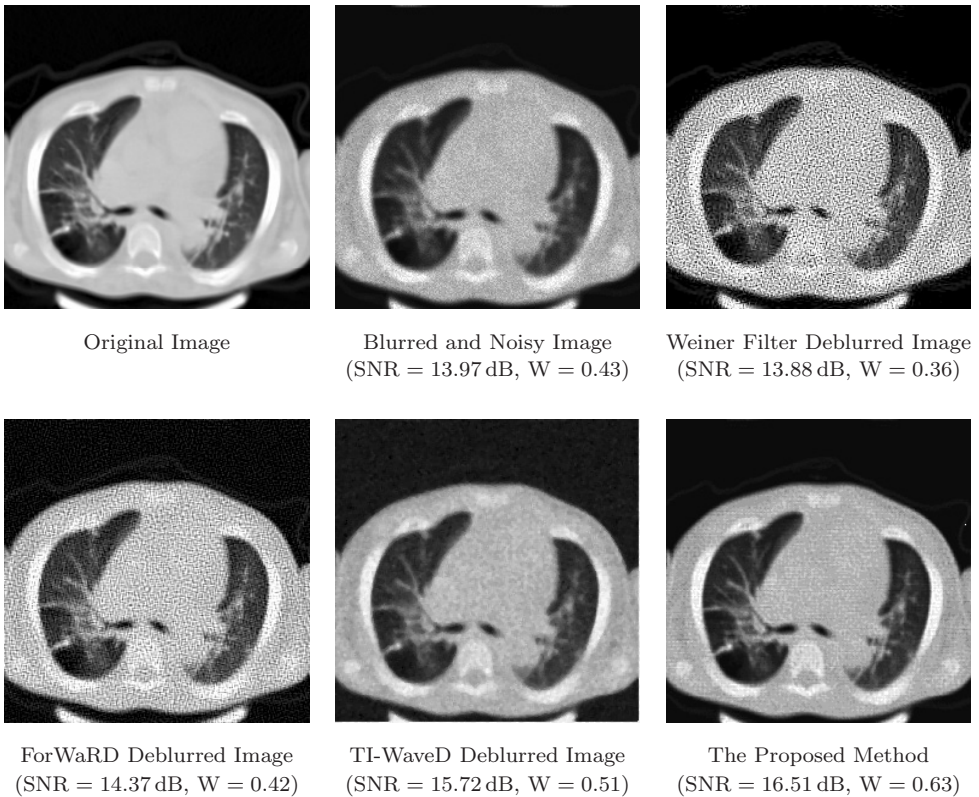


Fig. 4. Visual performance of the proposed method, compared to other methods.

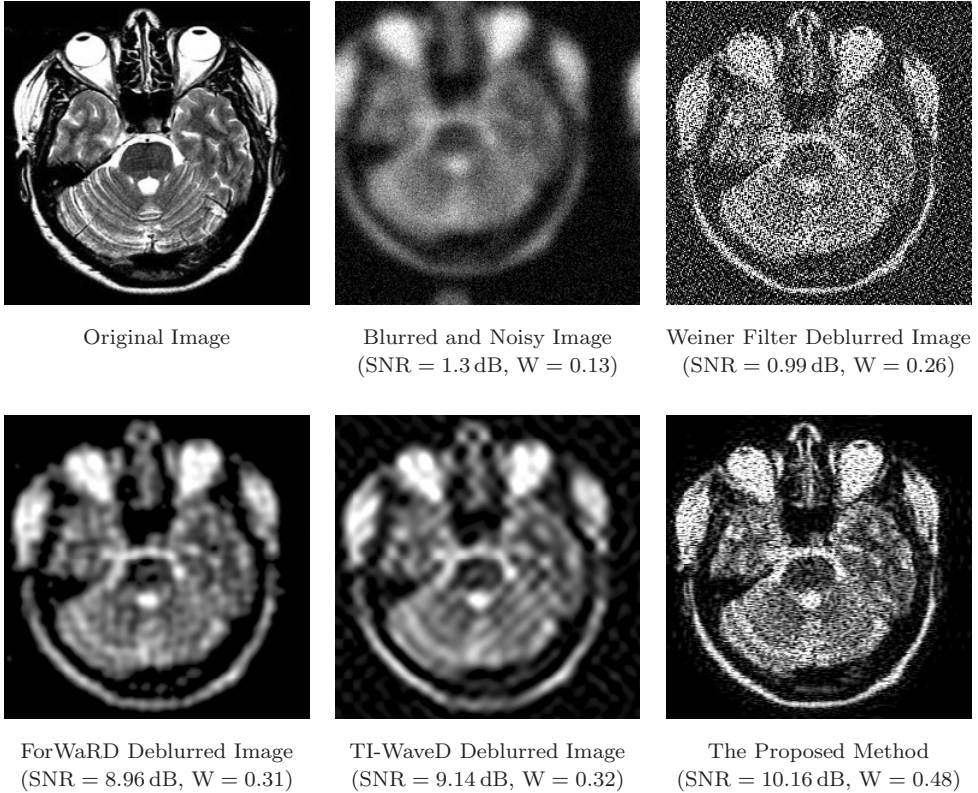


Fig. 5. Visual performance of the proposed method, compared to other methods on a blurred image corrupted by heavy noise.

we have done shrinkage upto the 8th level and used SDW14 complex wavelet, as it has been reported⁷ that it is an optimal choice for denoising. Figure 5 shows the superiority of the proposed method over others when the blurred image is corrupted by heavy amount of noise (SNR = 1.3 dB).

Table 1 present the results for deblurring of three different test blurred and noisy diagnostic images. The wavelet based performance measure (W) and SNR have been used for comparison of results in Table 1.

Figure 6 shows the plot of the mean square error (MSE) of noisy and blurred image with MSE of images deblurred by the proposed method as well as TI-WaveD, ForWaRD and the Wiener filter. Here in this experiment we have taken a combination of Uniform, Boxcar and Gaussian blurs and noise as combination of Gaussian additive, speckle and impulsive noise. These results clearly demonstrate the superiority of the proposed method over others. The results for the presence of specific types of noise in blurred images are shown in the Tables 2 and 3 in terms of SNR values. Here a test diagnostic image has been taken and blurred by various types of blur and different amounts of noise were added.

Table 1.

	Blurred Image	Weiner Filter Restored	ForWaRD Restored	TI-WaveD Restored	The Proposed Method
(A) Value of wavelet based blur measure (W) of different deblurred images.					
Test Image 1	0.26	0.31	0.37	0.41	0.45
Test Image 2	0.32	0.37	0.41	0.43	0.44
Test Image 3	0.47	0.52	0.59	0.65	0.69
(B) SNR value (in dB) of different deblurred images.					
Test Image 1	08.3214	08.9451	10.1098	12.0456	12.0952
Test Image 2	10.5913	11.6710	13.3534	14.9254	15.1878
Test Image 3	14.8046	15.8227	17.0473	17.8649	18.1772

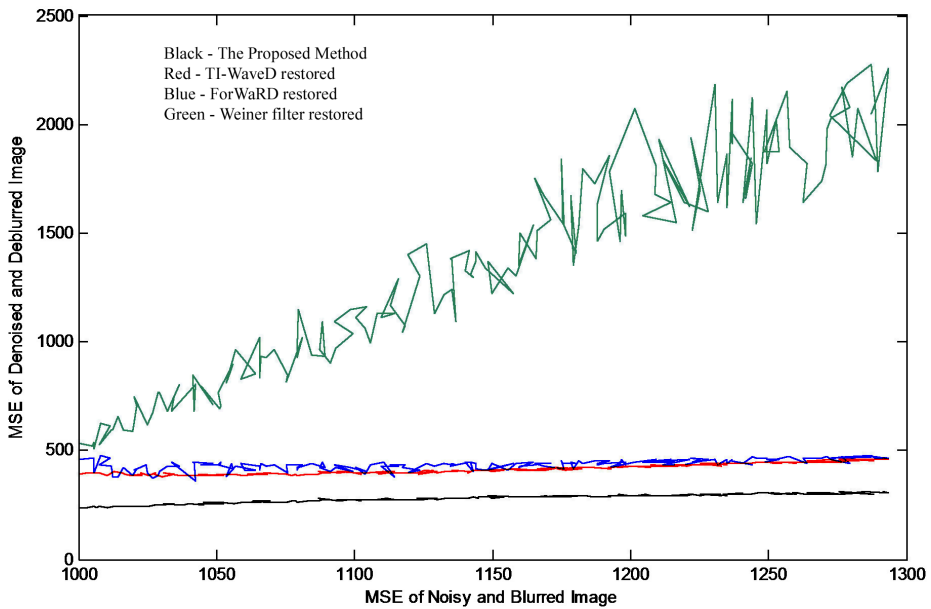


Fig. 6. MSE performance of the proposed method with TI-WaveD, ForWaRD and Weiner filter.

From the results presented in Table 2 it is clear that the performance of the proposed method is better than that of ForWaRD, TI-WaveD and the Weiner filter, for image having any type of blur and corrupted by signal dependent speckle noise.

The results presented in Table 3 indicate that for the image corrupted by signal independent Gaussian noise and having uniform blur, the proposed method is better at medium noise level while at low and high noise levels, TI-WaveD is better. Performance of the proposed method is also better at low and medium noise level for the images having Gaussian blur, while at high noise level TI-WaveD is better. In the presence of boxcar blur, at low noise level ForWaRD is better, at medium noise level the proposed method is better and at the high noise level TI-WaveD is better.

Table 2. Deblurring results of blurred image corrupted with speckle noise in term of SNR (in dB).

Noise Density (d)	Blurred Image	Weiner Filter Restored	ForWaRD Restored	TI-WaveD Restored	The Proposed Method
(A) Blurred image corrupted by uniform blur.					
Low Noise ($d = 0.001$)	11.8571	11.8026	12.6670	12.8101	15.1729
Medium Noise ($d = 0.05$)	10.0059	9.9010	10.4957	10.7910	12.4987
High Noise ($d = 0.4$)	9.1091	9.2317	10.5639	11.8845	12.0013
(B) Blurred image corrupted by Gaussian blur.					
Low Noise ($d = 0.001$)	14.7340	15.9648	17.9999	18.1934	18.6183
Medium Noise ($d = 0.05$)	11.7403	11.2830	13.4201	13.8733	14.8201
High Noise ($d = 0.4$)	9.1350	8.9800	11.5620	11.6999	12.1104
(C) Blurred image corrupted by boxcar blur.					
Low Noise ($d = 0.001$)	16.8357	17.7274	18.8956	18.2410	19.1610
Medium Noise ($d = 0.05$)	13.7403	13.8560	16.0139	16.3717	16.5610
High Noise ($d = 0.4$)	10.4327	10.0729	11.6671	12.3795	12.9903

Table 3. Deblurring results of blurred image corrupted with Gaussian noise in term of SNR (in dB).

Noise Variance (σ_{noise})	Blurred Image	Weiner Filter Restored	ForWaRD Restored	TI-WaveD Restored	The Proposed Method
(A) Blurred image corrupted by uniform blur.					
Low Noise ($\sigma_{\text{low}} = 0.05$)	11.4950	12.3418	13.3889	15.2349	14.6358
Medium Noise ($\sigma_{\text{med}} = 0.5$)	9.1243	9.3749	11.9755	12.9186	12.9659
High Noise ($\sigma_{\text{high}} = 1.0$)	8.2342	7.5817	10.5961	11.1141	11.0963
(B) Blurred image corrupted by Gaussian blur.					
Low Noise ($\sigma_{\text{low}} = 0.05$)	12.8745	13.5883	14.1306	14.4175	16.3515
Medium Noise ($\sigma_{\text{med}} = 0.5$)	10.5431	10.8405	12.1323	13.1752	14.1005
High Noise ($\sigma_{\text{high}} = 1.0$)	9.0543	9.9732	10.6117	11.4872	11.1894
(C) Blurred image corrupted by boxcar blur.					
Low Noise ($\sigma_{\text{low}} = 0.05$)	12.0159	13.7430	16.6145	14.4112	15.1698
Medium Noise ($\sigma_{\text{med}} = 0.5$)	9.7340	10.6470	12.6594	11.8326	13.4972
High Noise ($\sigma_{\text{high}} = 1.0$)	8.2432	8.2146	10.3150	11.8777	10.6297

Although the proposed method is far better than the Weiner filter, ForWaRD and TI-WaveD. However, here it is necessary to mention that deblurring in the presence of noise adds some artifacts in the image, which cannot be completely removed by the proposed method as well as other methods. However, Figs. 4 and 5 support the fact that the artifacts added are quite less in case of the proposed method compared to those of other methods.

5. Conclusions

Deblurring of blurred image in presence of noise is always a great challenge, because the removal of blur converts part of noise into colored noise. In this paper, we

addressed this issue and presented a new, robust and efficient complex wavelet domain deblurring method in presence of noise. The presented method first applies pseudo inverse filtering in complex wavelet domain on blurred and noisy image. Application of pseudo inverse filter removes blur, but adds colored noise, which is more difficult to remove. We have shown experimentally that the colored noise can be removed by applying multilevel soft-shrinkage in complex wavelet domain, using an adaptive level-dependent threshold, whose threshold value depends on the standard deviation of complex wavelet coefficients, the mean and the median of absolute complex wavelet coefficients, at a certain level. Application of multilevel shrinkage up to 7–10 levels gives good results. The proposed method is translation invariant due to use of Daubechies complex wavelet transform and can be applied to images having different types and amounts of blur and noise. The results presented in the paper demonstrate superiority of the proposed method over the Weiner filtering, ForWaRD and TI-WaveD.

Acknowledgments

This work was financially supported by the Korea Science and Engineering Foundation (KOSEF) grant (No. R01-2007-000-20227-0), and the systems biology infrastructure establishment grant provided by the Gwangju Institute of Science and Technology, Korea.

Appendix. The Soft Shrinkage Function

Wavelet coefficients of a noise free image are modeled as Gaussian.¹⁰ Figure 7 shows scatter plot of detailed complex wavelet coefficients of a noise free image. From this figure it is evident that the scatter plot is symmetric.

In most of the cases the noise can be modeled as additive and multiplicative noise or their combinations.⁶ Hence the general observation model in complex wavelet domain can be represented as,

$$w = \theta + n_G + n_S \quad (\text{A.1})$$

where, θ represents the wavelet coefficients of noise free image. n_G and n_S are the contributions to the wavelet coefficient due to Gaussian additive and speckle multiplicative noise. The distribution of Gaussian additive noise in wavelet domain is assumed to be zero-mean,

$$p(n_G) = \frac{1}{\sigma_{n_G} \sqrt{2\pi}} \exp\left\{-\frac{n_G^2}{2\sigma_{n_G}^2}\right\}. \quad (\text{A.2})$$

The distribution of speckle noise in wavelet domain can be modeled as Gamma distribution, as

$$p(n_S) = \frac{1}{\Gamma\lambda} (n_S)^{\lambda-1} \exp\{-n_S^2\}. \quad (\text{A.3})$$

We have observed that for fitting of actual wavelet coefficients of speckle noise to this model requires value of parameter λ to be positive odd integer greater than 2.

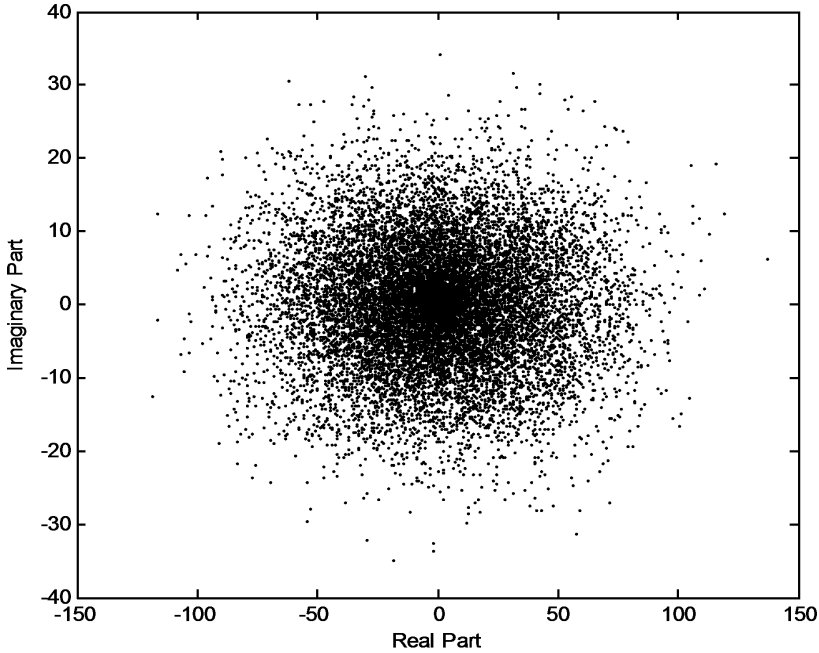


Fig. 7. Scatter plot of distribution of detailed Daubechies complex wavelet coefficients.

The objective is to estimate θ from known w . For this, Maximum *A Posteriori* (MAP) estimator is used as,

$$\hat{\theta} = \arg \max_{\theta} p(\theta|w)$$

using Bayes rule for conditional probability $p(\theta|w) = \frac{p(w|\theta)p(\theta)}{p(w)}$, so the MAP estimator becomes,

$$\hat{\theta} = \arg \max_{\theta} p(w|\theta)p(\theta)$$

or, after taking logarithm,

$$\hat{\theta} = \arg \max_{\theta} [\log p(w|\theta) + \log p(\theta)]. \tag{A.4}$$

The probability distribution of $w|\theta$ is the distribution of noise $n = w - \theta$ and since the wavelet coefficients of a noise free signal is modeled as a Gaussian distribution so,

$$p(\theta) = \frac{1}{\sigma\sqrt{2\pi}} \exp\left\{-\frac{\theta^2}{2\sigma^2}\right\}. \tag{A.5}$$

Let us estimate $\hat{\theta}$ for each case of noise with the help of a shrinkage function of the form $\hat{\theta} = f(\cdot)w$.

A.1. Estimation of $\hat{\theta}$

A.1.1. *Gaussian additive noise*

Since the distribution of noise is zero mean Gaussian in wavelet domain, as in Eq. (A.2), so

$$p(w|\theta) = \frac{1}{\sigma_{n_G} \sqrt{2\pi}} \exp\left\{-\frac{(w-\theta)^2}{2\sigma_{n_G}^2}\right\}. \tag{A.6}$$

Substituting this into MAP for $\hat{\theta}$ in Eq. (A.4),

$$\hat{\theta} = \arg \max_{\theta} \left[\log \frac{1}{\sigma_{n_G} \sqrt{2\pi}} \exp\left\{-\frac{(w-\theta)^2}{2\sigma_{n_G}^2}\right\} + \log \frac{1}{\sigma \sqrt{2\pi}} \exp\left\{-\frac{\theta^2}{2\sigma^2}\right\} \right]$$

or,

$$\hat{\theta} = \arg \max_{\theta} \left[\log \frac{1}{\sigma_{n_G} \sqrt{2\pi}} + \log \frac{1}{\sigma \sqrt{2\pi}} - \frac{(w-\theta)^2}{2\sigma_{n_G}^2} - \frac{\theta^2}{2\sigma^2} \right].$$

For a maximum value of θ

$$\frac{d}{d\theta} \left[-\frac{(w-\theta)^2}{2\sigma_{n_G}^2} - \frac{\theta^2}{2\sigma^2} \right] = 0$$

or,

$$\frac{2(w-\theta)}{2\sigma_{n_G}^2} - \frac{2\theta}{2\sigma^2} = 0$$

and after solving we get

$$\hat{\theta} = \frac{\sigma^2}{\sigma^2 + \sigma_{n_G}^2} w \tag{A.7}$$

here $f(\cdot) = f(\sigma) = \frac{\sigma^2}{\sigma^2 + \sigma_{n_G}^2}$.

A.1.2. *Speckle noise*

Distribution of speckle noise in wavelet domain is given by Eq. (A.3), so

$$p(w|\theta) = \frac{1}{\Gamma\lambda} (w-\theta)^{\lambda-1} \exp\{-(w-\theta)^2\}. \tag{A.8}$$

Substituting this into MAP for $\hat{\theta}$ in Eq. (A.4), we get

$$\hat{\theta} = \arg \max_{\theta} \left[\log \frac{1}{\Gamma\lambda} (w-\theta)^{\lambda-1} e^{-(w-\theta)^2} + \log \frac{1}{\sigma \sqrt{2\pi}} e^{-\theta^2/2\sigma^2} \right]$$

or,

$$\hat{\theta} = \arg \max_{\theta} \left[\log \frac{1}{\Gamma\lambda} + \log \frac{1}{\sigma \sqrt{2\pi}} + \log(w-\theta)^{\lambda-1} - (w-\theta)^2 - \frac{\theta^2}{2\sigma^2} \right]$$

or for a maximum value,

$$\frac{d}{d\theta} \left[\log(w-\theta)^{\lambda-1} - (w-\theta)^2 - \frac{\theta^2}{2\sigma^2} \right] = 0$$

or,

$$-\frac{\lambda - 1}{w - \theta} + 2(w - \theta) - \frac{\theta}{\sigma^2} = 0$$

gives,

$$(2\sigma^2 + 1)\theta^2 - (4\sigma^2 + 1)w\theta + (2w^2 + 1 - \lambda)\sigma^2 = 0,$$

solving this,

$$\hat{\theta} = \frac{(4\sigma^2 + 1)w \pm \sqrt{w^2 - 4\sigma^2(\lambda - 1)(2\sigma^2 + 1)}}{2(2\sigma^2 + 1)}. \tag{A.9}$$

Here $(\lambda - 1)$ is a positive constant and since at a particular level of wavelet coefficients, σ^2 is also a constant, therefore the term $4\sigma^2(\lambda - 1)(2\sigma^2 + 1)$ can be approximated by a constant k_1 , which depends on σ and in turn on w . Hence the term $\sqrt{w^2 - k_1}$ can be written as c_1w , for some chosen constant c_1 which depends on σ and λ . Thus,

$$\hat{\theta} = \frac{(4\sigma^2 + 1)w \pm c_1 \cdot w}{2(2\sigma^2 + 1)}. \tag{A.10}$$

Hence $\hat{\theta}$ may be expressed as $\hat{\theta} = f(\sigma)w$.

A.2. Soft-shrinkage function

For the Eq. (A.1),

$$\begin{aligned} \theta &= w - (n_G + n_S) \\ &= w - n_T \\ &= \left(1 - \frac{n_T}{w}\right)w \end{aligned} \tag{A.11}$$

where, n_T is the contribution of wavelet coefficients due to combination of various noise types. We found that the estimated value of θ is of the form, $\hat{\theta} = f(\cdot)w$, so the nature of $f(\cdot) = 1 - \frac{n_T}{w}$.

We have chosen the nature of $f(\cdot)$ as,

$$f(\cdot) = \frac{x^2}{x^2 + x_n^2} \tag{A.12}$$

where x and x_n are measurements of noise free signal and noise.

Solving it,

$$f(\cdot) = \frac{x^2}{x^2 + x_n^2} = \left(1 + \frac{x_n^2}{x^2}\right)^{-1} \approx 1 - \frac{x_n^2}{x^2}. \tag{A.13}$$

From Eqs. (A.11) and (A.13), our selected soft-shrinkage function based on idea of soft-thresholding is,

$$f(\sigma) = 1 - \frac{T^2}{w^2} \quad (\text{A.14})$$

where, T is threshold. If we restrict $f(\sigma) \in \{0, 1\}$, resulting in a soft-shrinkage function as,

$$f(\sigma) = \begin{cases} 0, & \text{if } |w| \leq T \\ \left(1 - \frac{T^2}{w^2}\right), & \text{if } |w| > T. \end{cases} \quad (\text{A.15})$$

References

1. O. Michailovich and D. Adam, Phase unwrapping for 2-D blind deconvolution of ultrasound images, *IEEE Trans. Medical Imaging* **23** (2004) 7–25.
2. F. C. Wagner, A. Macovski and D. G. Nishimura, A characterization of the scatter point-spread function in terms of air gaps, *IEEE Trans. Medical Imaging* **7** (1988) 337–344.
3. B. T. A. McKee, A. T. Gurvey, P. J. Harvey and D. C. Howse, A deconvolution scatter correction for a 3-D PET system, *IEEE Trans. Medical Imaging* **11** (1992) 560–569.
4. J. C. Yanch, M. A. Flower and S. Webb, A comparison of deconvolution and windowed subtraction techniques for scatter compensation in SPECT, *IEEE Trans. Medical Imaging* **7** (1988) 13–20.
5. M. Jiang, G. Wang, M. W. Skinner, J. T. Rubinstien and M. W. Vannier, Blind deblurring of spiral CT images, *IEEE Trans. Medical Imaging* **22** (2003) 837–845.
6. A. Khare and U. S. Tiwary, Soft-thresholding for denoising of medical images — A multiresolution approach, *Int. J. Wavelets Multiresolut. Inf. Process.* **3** (2005) 477–496.
7. A. Khare and U. S. Tiwary, Daubechies complex wavelet transform based technique for denoising of medical images, *Int. J. Image Graph.* **7** (2007) 663–687.
8. N. Kingsbury, Complex wavelets for shift invariant analysis and filtering of signals, *J. Appl. Computat. Harmon. Anal.* **10** (2001) 234–253.
9. F. C. A. Fernandes, R. L. C. Spaendonck and C. S. Burrus, A new framework for complex wavelet transform, *IEEE Trans. Signal Process.* **51** (2003) 1825–1837.
10. D. Clonda, J.-M. Lina and B. Goulard, Complex Daubechies wavelets: Properties and statistical image modeling, *Signal Process.* **84** (2004) 1–23.
11. I. W. Selesnick, R. G. Baraniuk and N. Kingsbury, The dual-tree complex wavelet transform — A coherent framework for multiscale signal and image processing, *IEEE Signal Process. Mag.* **22** (2005) 123–151.
12. D. L. Donoho and M. Raimondo, Translation invariant deconvolution in a periodic setting, *Int. J. Wavelets Multiresolut. Inf. Process.* **2** (2004) 415–432.
13. Q. Gao, D. Zhang and Y. Wang, Speckle reduction in polarimetric SAR imagery combining by PWF and stationary wavelet thresholding, *Int. J. Wavelets Multiresolut. Inf. Process.* **4** (2006) 589–599.
14. R. A. Gopinath, The phaselet transform — An integral redundancy nearly shift-invariant wavelet transform, *IEEE Trans. Signal Process.* **51** (2003) 1792–1805.
15. J. Neumann and G. Steidl, Dual-tree complex wavelet transform in the frequency domain and an application to signal classification, *Int. J. Wavelets Multiresolut. Inf. Process.* **3** (2005) 43–65.

16. L. Peng and W. Yuan, Higher-density dual tree discrete wavelet transform, *Int. J. Wavelets Multiresolut. Inf. Process.* **5** (2007) 815–841.
17. A. A. Bharath and J. Ng, A Steerable complex wavelet construction and its application to image denoising, *IEEE Trans. Image Process.* **14** (2005) 948–959.
18. W. Lawton, Applications of complex valued wavelet transform in subband decomposition, *IEEE Trans. Signal Process.* **41** (1993) 3566–3568.
19. J.-M. Lina and M. Mayrand, Complex Daubechies wavelets, *J. Appl. Computat. Harmon. Anal.* **2** (1995) 219–229.
20. D. L. Donoho, Nonlinear solution of linear inverse problems by wavelet-vaguelette decomposition, *Appl. Computat. Harmon. Anal.* **2** (1995) 101–126.
21. J. Kalifa, S. G. Mallat and B. Rouge, Minimax solution of inverse problems and deconvolution by mirror wavelet thresholding, *Proc. SPIE* **3813** (1999) 42–57.
22. J. Kalifa and S. Mallat, Thresholding estimators for linear inverse problems and deconvolutions, *Ann. Statist.* **31** (2003) 58–109.
23. J. Fan and J. Koo, Wavelet deconvolution, *IEEE Trans. Inform. Theory* **48** (2002) 734–747.
24. P. Guo, H. Li and M. R. Lyu, Blind image restoration by combining wavelet transform and RBF neural network, *Int. J. Wavelets Multiresolut. Inf. Process.* **5** (2007) 15–26.
25. R. Neelamani, H. Choi and R. Baranick, ForWaRD: Fourier — Wavelet regularized deconvolution for ill-conditioned systems, *IEEE Trans. Signal Process.* **52** (2004) 418–433.
26. M. Li, B. Hao and X. Feng, Iterative regularization and nonlinear inverse scale space based on translation invariant wavelet shrinkage, *Int. J. Wavelets Multiresolut. Inf. Process.* **6** (2008) 83–95.
27. I. M. Johnstone, G. Kerkycharian, D. Picard and M. Raimondo, Wavelet deconvolution in a periodic setting, *J. Roy. Statist. Soc. Ser. B* **66** (2004) 547–573.
28. I. Daubechies, *Ten Lectures on Wavelets* (SIAM, 1992).
29. A. Khare and U. S. Tiwary, Daubechies complex wavelet transform based moving object tracking, in *Proc. IEEE Symposium on Computational Intelligence in Image and Signal Processing*, Honolulu, Hawaii, USA (2007), pp. 36–40.
30. L. Bar, N. Sochen and N. Kiryati, Image deblurring in the presence of salt-and-pepper noise, image processing, in *Scale Space 2005*, eds. R. Kimmel, N. Sochen and J. Weickert, Lecture Notes in Computer Science, Vol. 3459 (Springer, 2005), pp. 107–118.
31. A. Jalobeanu, L. Blanc-Feraud and J. Zerubia, Satellite image deconvolution using complex wavelets packets, Report No. 3955, Inst. Nat. de Recherche en Informatique et Automatique (INRIA), Sophia, Antipolis, Cedex-France (2000).
32. J. Kautsky, J. Flusser, B. Zitova and S. Simberova, A new wavelet-based measure of image focus, *Pattern Recogn. Lett.* **23** (2002) 1785–1794.
33. A. K. Jain, *Digital Image Processing* (Prentice Hall of India, 1989).
34. Z. Huang, B. Fang, X. He and L. Xia, Image denoising based on the dyadic wavelet transform and improved threshold, *Int. J. Wavelets Multiresolut. Inf. Process.* **7** (2009) 269–280.
35. D. Cho, T. D. Bui and G. Chen, Image denoising based on wavelet shrinkage using neighbor and level dependency, *Int. J. Wavelets Multiresolut. Inf. Process.* **7** (2009) 299–311.